"This is an Accepted Manuscript of an article published by Industrial & Engineering Chemistry Research (I & ECR), doi: 10.1021/acs.iecr.8b01424, accepted in June 2018; vol 57, 8664-8678 (2018)."

'Optimulation' in Chemical Reaction Engineering: The Oxidative Coupling of Methane as a Case Study

Yousef Mohammadi[1]* and Alexander Penlidis[2]*

[1]Petrochemical Research and Technology Company (NPC-rt), National Petrochemical Company (NPC), P.O. Box 14358-84711, Tehran, Iran

[2]Department of Chemical Engineering, Institute for Polymer Research (IPR), University of Waterloo, Waterloo, Ontario N2L 3G1, Canada

* To whom correspondence should be addressed:

Dr. Yousef Mohammadi: mohammadi@npc-rt.ir

Prof. Alexander Penlidis: penlidis@uwaterloo.ca

Phone: 519 888 4567 ext 36634

ABSTRACT

The optimization of reacting systems, including chemical, biological, and macromolecular reactions, is of great importance from both theoretical and practical standpoints. Even though several classical deterministic and stochastic modeling and simulation approaches have been routinely examined to understand and control reacting systems from lab- to industrial-scales, almost all tackling the same problem, i.e., how to predict reaction outputs from any given set of reaction input variables. Development and application of an effective and versatile mathematical tool capable of appropriately connecting preset desired reaction outputs to corresponding inputs have always been the ideal goal for experts in the related fields. Hence, there definitely exists the need to predict a priori optimum reaction conditions in a computationally-demanding multi-variable space for both keeping the chemical and biological reactions in optimal conditions and at the same time satisfying preset desired targets. As a novel and powerful solution, we hereby introduce a robust and functional computational tool capable of simultaneously simulating and optimizing, i.e. 'optim-ulating' intricate chemical, biological, and macromolecular reactions via the amalgamation of the Kinetic Monte Carlo (KMC) simulation approach and the multi-objective version of Genetic Algorithms (NSGA-II). The synergistic interplay of KMC and NSGA-II for the optimulation of Oxidative Coupling of Methane (OCM) as an example of a challenging chemical reaction engineering system has clearly demonstrated the outstanding capabilities of the proposed method. Undoubtedly, the proposed novel hybridized technique is very powerful and can address a variety of unsolved optimization questions in chemical, biological, and macromolecular reaction engineering.

Keywords: Computational Intelligence; OCM; Reaction Engineering; Optimization; Kinetic Monte Carlo; Simulation

1. INTRODUCTION

Reacting systems of both scientific and practical interest are generally very complicated. They usually comprise a large number of distinct elementary reactions, mainly with rate constants differing by several orders of magnitude, frequently with surface reaction and additional transport steps. Hence, Chemical Reaction Engineering, the field of establishing proper and reliable mechanisms capable of appropriately describing the behavior of a reacting system, is of great importance and can be extremely cumbersome.

Simulation and optimization are effective mathematical tools in treating intricate reaction engineering problems. The former is an essential computational technique to reveal complex interrelationships between reaction inputs and outputs, while the latter is of paramount importance in order to minimize energy and raw material consumption and at the same time maximize productivity and improve product quality. In the last few decades, several classical deterministic and stochastic modeling and simulation approaches (and also the related software packages) have been successfully developed and put into practice to identify the behavior of reacting systems (for a sample of typical applications, see references (1)-(9)). Among these approaches, molecular simulation techniques, which are powerful and versatile computational tools, have become the focus of attention in recent years. Considering their outstanding capabilities, various molecular simulation methods for studying materials and reactions at the atomic level (Quantum Mechanics, Molecular Dynamics, and Monte Carlo approaches) have been reviewed in references (10)-(14).

Nowadays, the Kinetic Monte Carlo (KMC) approach has almost become a standard stochastic molecular simulation tool, widely employed for simulating complex reacting systems.[15-17] KMC is capable of simulating molecular reactions via a computer version of the reaction in a virtual reactor. In other words, virtual molecules react with each other through well-established digital reaction channels in a pre-determined order governed by instantaneous reaction rates.

KMC makes 'digital synthesis' possible via computer codes composed of well-defined reactants, reaction schemes, reaction kinetics, and related rate law functions. It has already been successfully applied in a large variety of chemical, biological, and macromolecular reaction engineering fields.[18-23] Taking into consideration KMC's outstanding capabilities in tracking each reactant over the reaction course, one can find it powerful enough to uncover many of the complexities and unobservable details in reacting systems. Undoubtedly, high computational cost is one of the major disadvantages of KMC simulations, which can be effectively improved by the development of sophisticated computer codes and computationally fast algorithms.[24-29] The developed codes should have functional data storage structures and also establish a suitable interplay among the CPU, RAM, and Hard Disk of the computer. Despite many remarkable capabilities, still lacking in KMC simulators is their inability to discover the complex interrelationships among input variables (e.g. operational and compositional parameters or reactor configuration and mode of operation) and outputs (e.g. conversion, selectivity, property distributions, and yield). While in practice the prediction of inputs for a set of predefined targets is of great importance, the conventional KMC simulators are only 'expert' in revealing the reaction outputs from a given set of input reaction variables. In other words, KMC simulators intrinsically cannot be applied for optimization purposes.

To equip the KMC simulator with both simulation and optimization capabilities, i.e. determining appropriate input variables resulting in predefined targets, it is essential to design a robust version of KMC simulators with the capability for seeking and screening all possible reaction recipes and identifying complex, non-linear interrelationships among input variables and reaction outputs. In fact, the simulator should be provided with appropriate optimization tools to have the opportunity to intelligently explore the reaction search space in an attempt to find optimum recipes (i.e. optimal input values) for complex reacting systems resulting in predefined reaction outputs (e.g. preset conversion, yield and/or other product properties).

Nowadays, Artificial Intelligence techniques are of vital importance in Applied Sciences and Engineering, and undoubtedly play a key role in everyday life.[30-32] Basically, all Intelligent Computation techniques are equipped with critical components of 'intelligence', including learning, generalization, and decision-making for modeling and optimization of complex nonlinear phenomena.[33] Artificial Neural Networks and Fuzzy Logic Systems are the most powerful intelligent modelers, whereas intelligent optimizers include Swarm Intelligence, Simulated Annealing, and Genetic Algorithms. Artificial Intelligence techniques are the most versatile and effective stochastic modeling and optimization tools successfully employed in different fields of science and technology.[34-38] Generally speaking, Artificial Neural Networks (ANNs), as biologically inspired modeling tools, and Genetic Algorithms (GAs), as evolutionary optimization algorithms, have frequently been utilized for modeling and optimization of a large variety of phenomena in different fields.[39-41] Indeed, the potential advantages of Intelligent Computation techniques in KMC simulations can be very beneficial and challenging. Hence, proper implementation and amalgamation of Artificial Intelligence techniques with the KMC approach could effectively address weaknesses associated with KMC simulators (as discussed above). We hereby introduce this new concept as the 'optimulation' algorithm. In fact, 'optimulation' synergistically combines the beneficial features of both the KMC simulation method and intelligent optimization techniques.

In the current study, the proposed 'optimulation' algorithm is implemented to 'optimulate' the Oxidative Coupling of Methane (OCM) as a complex chemical reaction case study. To do this, a well-designed KMC simulator is established by computer programming to virtually imitate the OCM process. Afterwards, an appropriate Artificial Intelligence technique, the Non-dominated Sorting Genetic Algorithm (NSGA-II), is amalgamated with the developed KMC simulator to predict the optimal input variables resulting in predefined reaction outputs.

2. MODEL DEVELOPMENT

A two-stage stochastic computational approach is required for successful implementation of the optimulation methodology. Firstly, a digital version of the reaction should be developed by computer programming applying KMC simulation concepts. Taking as many possible details into account, the digital synthesizer (molecular simulator) must be capable of virtually mimicking the real reacting system via predefined reaction channels and also calculating/reporting the reaction outputs. To guarantee the success of optimulation, an accurate and computationally cost-effective KMC simulator should be available.

In the second stage, an optimizer capable of exploring the reaction search space in an intelligent evolutionary manner should be developed and appropriately hybridized with the KMC simulator. The interplay between the KMC simulator and intelligent optimizer decodes the complex interrelationships between input factors and reaction outputs. In fact, the intelligent optimizer (a powerful and versatile heuristic search strategy) generates numerous reaction recipes. Then, it recalls the KMC simulator as frequently as needed in order to run the virtual reactor for each recipe one by one, and subsequently stores the reaction outputs for all recipes separately. Hence, following this strategy, each reaction recipe (a genotype) is precisely connected to a set of reaction outputs (its phenotype).

To illustrate the capabilities of the proposed optimulation algorithm, it has been applied to the challenging, multi-objective optimization of oxidative coupling of methane or OCM, a complex chemical reaction engineering problem. In the following subsections, the implementation of the algorithm is comprehensively described for ‘optimulating’ the OCM process.

2.1. Stage I: Development of the KMC simulator for the reacting system

Ethylene is one of the most important primary building blocks, with a worldwide production capacity of 170 million metric tonnes per year in 2016 and also with an

estimated annual production capacity of over 230 million metric tonnes in 2025.[42,43] Nowadays, it is industrially utilized for polymerization to polyethylene, oxidation to ethylene oxide, oligomerization to form other olefins, and halogenation to vinyl chloride. Around 90% of ethylene is directly consumed to produce chemicals like ethylene oxide and polyethylene, which are subsequently utilized in the production of detergents, surfactants, and different packaging materials.[44] In the United States, 70% of all ethylene is produced via thermal cracking, heating light hydrocarbons to 750-950°C.[45] These high temperatures break the large hydrocarbons into smaller ones through free radical reactions. Ethylene is then separated and extracted from the mixture with compression and distillation.

Over the past few decades, various direct and indirect methods have been examined for methane (CH_4) conversion into more useful products, including olefins (e.g. C_2H_4, C_3H_6), higher hydrocarbons, and liquids (e.g. benzene and gasoline).[46-48] The oxidative coupling of methane, a prospective route for the utilization of natural gas as a chemical and petrochemical feedstock, has been the target of enormous theoretical and practical interest for more than thirty years due to the large potential of the process to reduce cost, energy, and environmental emissions during the production of useful chemicals, especially ethylene. Interestingly, the coupling of methane in the absence of oxygen is extremely endothermic and the conversion is very limited, due to thermodynamic limits. The process is exothermic in the presence of oxygen (Equation 1).[49-51] It is worth mentioning that both partial and total oxidations are favored in the OCM process due to thermodynamic reasons (Equations 2 and 3).[52] Hence, catalysts are used to achieve a reasonable yield. In the OCM process, methane and oxygen react over a catalyst exothermically to form ethylene, water, and heat.

Overall Pathway: $2CH_4 + O_2 \rightarrow C_2H_4 + 2H_2O \quad \Delta H_r(800°C) = -139\ kJ/mol$ (1)

Partial Oxidation: $CH_4 + \frac{3}{2}O_2 \rightarrow CO + 2H_2O \quad \Delta H_r(800°C) = -519\ kJ/mol$ (2)

Total Oxidation: $2CH_4 + 2O_2 \rightarrow CO_2 + 2H_2O \quad \Delta H_r(800°C) = -801\ kJ/mol$ (3)

Despite intensive efforts on the OCM process, there are still serious problems related to the commercialization of this technology. This is mainly due to the fact that the intermediates and desired products (i.e. C_2 hydrocarbons) are usually more reactive than the raw material (methane), and therefore prone to partially or totally oxidize to carbon mono- and di-oxide.[52] From both scientific and commercial standpoints, control and optimization of the OCM process (a multi-objective problem) is of paramount importance and definitely requires the development and application of powerful mathematical tools. To construct the KMC simulator virtually resembling the OCM process, the comprehensive 10-step kinetic model including nine catalytic reactions and one gas phase reaction proposed by Stansch et al.[53] for the oxidative coupling of methane to C_{2+} hydrocarbons was utilized (see Scheme 1). This scheme explains the differential rates of formation of different species in the La_2O_3/CaO packed bed reactor under a wide range of experimental conditions. The gas feed contains O_2 and CH_4 as reactants and is diluted with N_2. Also, eight species including C_2H_4, C_2H_6, CH_4, CO_2, CO, O_2, H_2O and H_2 participate in the reaction network.

Although several reaction schemes have been proposed to study the kinetics of OCM process, almost all of them have employed the kinetic model of Scheme 1 as the main framework, with some modifications (e.g. see references (54)-(59)). The proposed kinetic model includes (1) thermal cracking, (2) steam reforming, and (3) water-gas shift reactions. According to this reaction scheme, methane is allowed to be converted via three parallel primary reaction channels including (i) nonselective total oxidation of methane to carbon dioxide (step 1), (ii) formation of ethane by oxidative coupling of methane (step 2), and also (iii) partial oxidation of methane to carbon monoxide (step 3). Furthermore, carbon monoxide could react with oxygen and convert to carbon dioxide (step 4) which is coupled with the water-gas shift reaction in both directions (steps 9 and 10). In the other steps, ethane can be converted by two parallel routes, i.e. by heterogeneous catalytic oxidative dehydrogenation of ethane (step 5) and thermal gas-phase dehydrogenation of ethane to ethylene occurring under high temperature (step 7).

Finally, ethylene can be converted to carbon monoxide in two parallel ways, i.e. partial oxidation (step 6) and steam reforming (step 8).

Scheme 1. Reaction scheme applied for KMC simulation of OCM process.[53]

Step	Reaction Channel
Step 1	$CH_4 + 2O_2 \rightarrow CO_2 + 2H_2O$
Step 2	$2CH_4 + 0.5O_2 \rightarrow C_2H_6 + H_2O$
Step 3	$CH_4 + O_2 \rightarrow CO + H_2O + H_2$
Step 4	$CO + 0.5O_2 \rightarrow CO_2$
Step 5	$C_2H_6 + 0.5O_2 \rightarrow C_2H_4 + H_2O$
Step 6	$C_2H_4 + 2O_2 \rightarrow 2CO + 2H_2O$
Step 7	$C_2H_6 \rightarrow C_2H_4 + H_2$
Step 8	$C_2H_4 + 2H_2O \rightarrow 2CO + 4H_2$
Step 9	$CO + H_2O \rightarrow CO_2 + H_2$
Step 10	$CO_2 + H_2 \rightarrow CO + H_2O$

Figure 1 schematically represents the reactor configuration applied to study the kinetics of OCM process.[52,53] As can be observed, the reactor is composed of three distinct segments, including an upstream part, a catalytic fixed bed part, and a downstream part. It should be noted that the inner tube diameter (*ID*), bed porosity (ε), and bed density (ρ) are set to be 6 mm, 0.5, and 130 kg/m^3, respectively.[52] The height of the catalytic packed bed varies depending on the modified reaction time, *MRT* (kg.s.m^{-3}), as follows:

$$MRT = \frac{M_{cat}}{\dot{V}_{gas}} \tag{2}$$

where M_{cat} denotes the total mass of the catalyst in the reactor (kg) and $\mathring{V}_{gas}$ is the volumetric flow of the gas (m^3.s^{-1}).

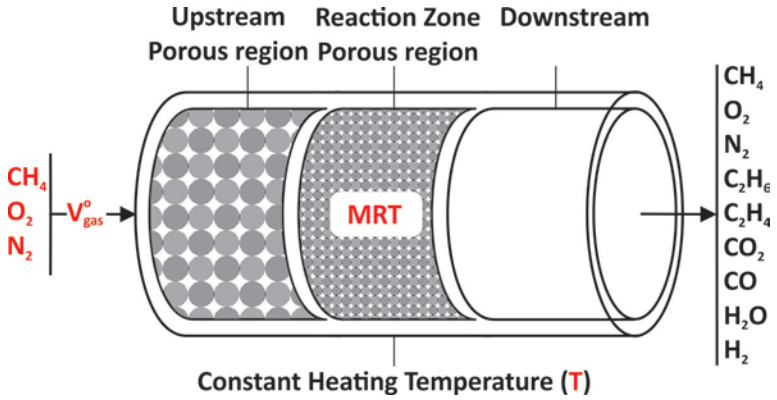

Figure 1. Schematic representation of the reactor configuration for OCM process.

Following the work in references (52)-(53), several reaction factors of interest (input variables) are selected as regulating factors in the optimulation algorithm. The selected factors (to be adjusted) permit manipulation of the reacting system and investigation of the influences of either a factor individually or several factors simultaneously by the developed KMC simulator (thus leading to complex single- and multi-objective optimization problems). The manipulated reaction inputs include (1) modified reaction time (MRT), (2) volumetric flow of the gas ($\mathring{V}_{gas}$), (3) inlet methane to oxygen ratio (X_{CH4}/X_{O2}), (4) inlet mole fraction of nitrogen (X_{N2}), and (5) reaction temperature (T). Methane conversion (CH_4 conversion), C_2 selectivity (S_{C2+}), and C_2 yield (Y_{C2+}) are considered the main reaction outputs of interest. These can be calculated as follows:

$$CH_4\ conversion = \frac{moles\ of\ CH_4\ converted}{(moles\ of\ CH_4)_{Feed}} \times 100 \tag{3}$$

$$S_{C2+} = \frac{\sum n(moles\ of\ C_n\ hydrocarbons)_{Products}}{(moles\ of\ CO + moles\ of\ CO_2 + \sum n(moles\ of\ C_n\ hydrocarbons))_{Products}} \tag{4}$$

$$Y_{C2+} = X_{CH_4} \times S_{C_{2+}} \tag{5}$$

The following reaction rates, reported by Stansch et al. (Equations 6-11) along with the kinetic parameters tabulated in Table 1, were applied to simulate the OCM process by the KMC approach.[53]

$$r_j = \frac{k_{0,j} e^{-E_{a,j}/RT} p_{O2}^{n_j} p_C^{m_j}}{\left[1 + K_{j,CO2} e^{-\Delta H_{ad,CO2,j}/RT} p_{CO2}\right]^2} \quad \text{(Steps 1 and 3-6)} \quad (6)$$

$$r_j = \frac{k_{0,j} e^{-E_{a,j}/RT} \left(K_{0,O2} e^{-\Delta H_{ad,O2}/RT} p_{O2}\right)^{n_j} p_{CH4}^{m_j}}{\left[1 + \left(K_{0,O2} e^{-\Delta H_{ad,O2}/RT} p_{O2}\right)^{n_j} + K_{j,CO2} e^{-\Delta H_{ad,CO2,j}/RT} p_{CO2}\right]^2} \quad \text{(Step 2)} \quad (7)$$

$$r_7 = k_{0,7} e^{-E_{a,7}/RT} p_{C_2H_6} \quad \text{(Step 7)} \quad (8)$$

$$r_8 = k_{0,8} e^{-E_{a,8}/RT} p_{C_2H_4}^{n_8} p_{H_2O}^{m_8} \quad \text{(Step 8)} \quad (9)$$

$$r_9 = k_{0,9} e^{-E_{a,9}/RT} p_{CO}^{n_9} p_{H_2O}^{m_9} \quad \text{(Step 9)} \quad (10)$$

$$r_{10} = k_{0,10} e^{-E_{a,10}/RT} p_{CO_2}^{n_{10}} p_{H_2}^{m_{10}} \quad \text{(Step 10)} \quad (11)$$

Table 1: Kinetic parameters for OCM by Stansch et al.[53]

Step	$K_{0,j}$ [mol/(g.s.Pa^{m+n})]	$E_{a,j}$ [kJ/mol]	$K_{j,CO2}$ [Pa^{-1}]	$\Delta H_{ad,CO2}$ [kJ/mol]	K_{O2} [Pa^{-1}]	$\Delta H_{ad,O2}$ [kJ/mol]	m_j	n_j
1	0.2×10^{-5}	48	0.25×10^{-12}	-175	-	-	0.24	0.76
2	23.2	182	0.83×10^{-13}	-186	0.23×10^{-11}	-124	1.0	0.40
3	0.52×10^{-6}	68	0.36×10^{-13}	-187	-	-	0.57	0.85
4	0.11×10^{-3}	104	0.40×10^{-12}	-168	-	-	1.0	0.55
5	0.17	157	0.45×10^{-12}	-166	-	-	0.95	0.37
6	0.06	166	0.16×10^{-12}	-211	-	-	1.0	0.96
7	1.2×10^{7}	226	-	-	-	-	1.0	-
8	9.3×10^{3}	300	-	-	-	-	0.97	0
9	0.19×10^{-3}	173	-	-	-	-	1.0	1.0
10	0.26×10^{-1}	220	-	-	-	-	1.0	1.0

In the present study, Gillespie's algorithm was implemented to develop and construct an appropriate simulator for the OCM process.[15] To do this, the simulation volume, *V*, was assumed to be shared homogeneously among the reactants. Accordingly, microscopic elementary reactions occurred discretely and stochastically through 10 reaction channels (see Scheme 1) and an event was selected in a given time interval (*t*, *t*+*dt*) from uniformly distributed random numbers in a unit interval, according to the following relationships:

$$\sum_{i=1}^{\mu-1} P_i < r_1 \leq \sum_{i=1}^{\mu} P_i \tag{12}$$

$$dt = \frac{1}{\sum_{i=1}^{10} R_i} \ln\left(\frac{1}{r_2}\right) \tag{13}$$

where r_1 and r_2 are two random numbers, μ is the number of the selected reaction channel (according to Scheme 1, it can be an integer between 1-10), *dt* is the time interval between two successive reactions, while P_i and R_i are the instantaneous reaction rate probability and rate of reaction *i*, respectively.

The rate of reaction *i* (i.e. R_i; *i* = 1, 2, 3 … 10) can be determined applying Equations 6-11. Also, the instantaneous reaction rate probability of reaction *i* can be calculated as follows:

$$P_i = \frac{R_i}{\sum_{j=1}^{10} R_j} \tag{14}$$

To construct the KMC simulator, the aforementioned input variables, including three compositional ($\mathring{V}_{gas}$, X_{CH4}/X_{O2}, and X_{N2}) and two operational (*MRT* and *T*) factors, were defined. Then, an appropriate function was defined/developed for each reaction channel capable of virtually resembling that channel. In fact, the virtual reactants can digitally react with each other according to the rules dictated by each reaction channel. Afterwards, the selected function adjusted the concentration of reactants accordingly. The simulation proceeded via frequently selecting the reaction channels based on the roulette wheel mechanism considering instantaneous reaction rates and updating the populations of reactants and products according to the stoichiometry of the selected channel. The KMC simulation flowchart for the OCM process is presented in Figure 2.

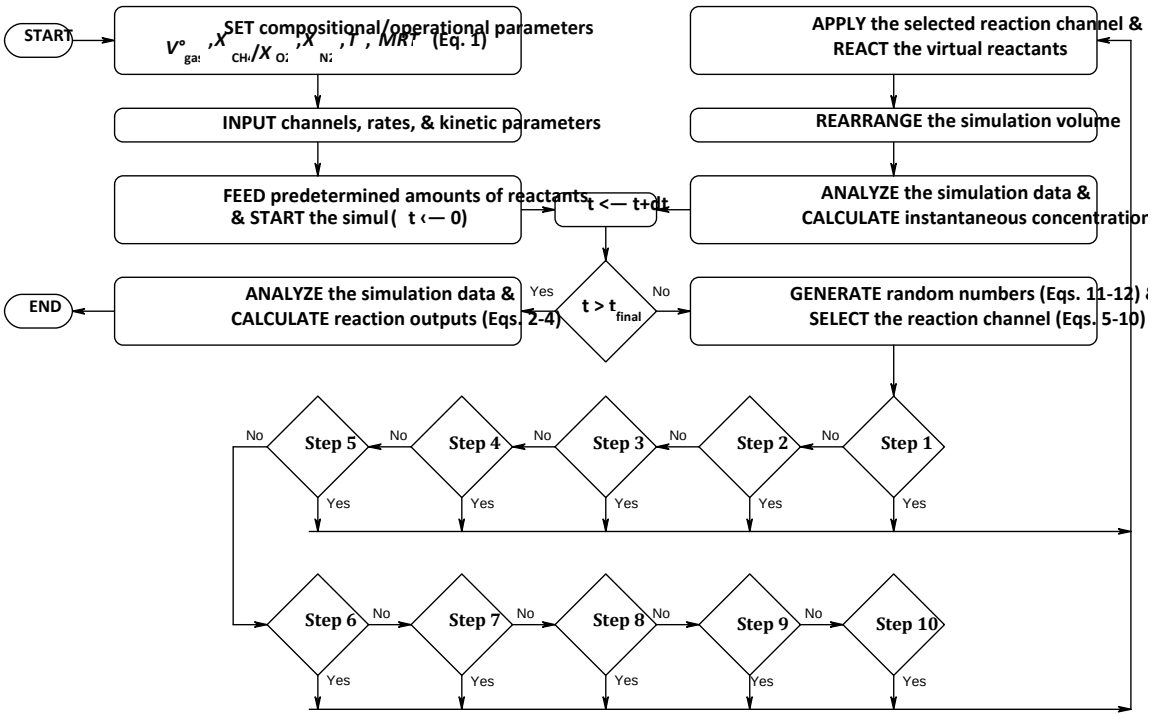

Figure 2. Flowchart applied to develop KMC simulator for OCM process.

A simulator, according to the aforementioned reaction scheme and flow chart presented in Figure 2, was written in Pascal programming language (Lazarus 1.6.4 IDE) and compiled into 64-bit executable using FPC 3.0.2. A subroutine based on the ‘‘Mother-of-all Pseudo Random number Generators’’ algorithm was utilized to produce the required random numbers for the simulation.[60] The random number generation subroutine satisfied the tests of uniformity and serial correlation with high resolution. The cycle length of the random number generator was 3×10^{47}. Simulations were performed on a desktop computer with Intel Core i7-3770K (3.50 GHz), 32 GB of memory (2133 MHz), under Windows 7 Ultimate 64-bit operating system. The runtime approximately took between 0.1 and 1.5 sec.

2.2. Stage II: Development of the intelligent optimizer

In the second stage of the optimulation algorithm, a powerful and versatile multi-objective optimizer capable of communicating with the KMC simulator should be developed based on Computational Intelligence techniques. Optimization of the OCM

process is a complex multi-objective problem (since many compositional and operational parameters concurrently influence the reacting system). Hence, the selection of an appropriate and powerful optimization tool is of vital importance to be hybridized with the well-developed KMC simulator and handle the optimulation process. As simultaneous satisfaction of several predefined objectives and constraints is necessary in complex reacting systems, a well-designed optimization tool for complex multi-objective problems should be employed.

In general, classical multi-objective optimization techniques, including weighted sum, goal programming, goal attainment, and ε-constraint, are mostly based on the decomposition concept. In fact, they transform a multi-objective optimization problem into several single-objective ones. Hence, they are not powerful enough to handle multi-objective problems, like complex chemical reactions, as they are not equipped with powerful searching and decision-making tools.[61] They basically apply deterministic transition principles to 'scalar-ize' iteratively multiple objectives in exploring a set of Pareto-optimal solutions. The fact is that the whole set of Pareto optimal solutions is not accessible in a single trial applying the mentioned traditional approaches. In other words, merely some of the optimal solutions are disclosed at any specific potential setting. Hence, they must be put into practice several times and each time the settings (i.e. the relevant built-in parameters of the algorithm) should be precisely altered/adjusted to obtain a part of the Pareto optimal solution. On the other hand, Computational Intelligence-based optimizations attempt to find solutions in an evolutionary single simulation trial, so that no other solutions in the search space dominate Pareto-optimal solutions of the dominated front.[62] In contrast to classical deterministic multi-objective optimization algorithms, stochastic evolutionary techniques such as NSGA-II are considerably more functional and computationally efficient alternatives.

Computational Intelligence techniques as stochastic modeling and optimization tools are able to learn, generalize, and make decisions (i.e. they enjoy all three principal components of intelligence).[63] Genetic Algorithms are the most popular intelligent optimization techniques widely applied in different fields of study due to simplicity,

flexibility, versatility, and high potential to handle a large variety of problems.[64-68] Genetic Algorithms, inspired by the process of natural selection, lead to heuristic search strategies. Randomly producing a population of potential solutions, they stochastically evolve it toward better solutions via the application of powerful genetic operators. Not only are Genetic Algorithms masterful in single-objective optimizations, but they are also capable of handling two or more objectives and constraints concurrently in complex multi-objective optimizations. Among different Genetic Algorithms, NSGA-II is a unique multi-objective version of the family established primarily based on the domination concept. Undoubtedly, it can be considered as one of the most popular multi-objective optimization techniques in different fields of science and technology.

In the current study, NSGA-II was put into practice to interact with the developed KMC simulator and handle the optimulation of the OCM process by satisfying several predefined objectives and constraints. Except for population sorting, NSGA-II follows all principal steps of single-objective versions of Genetic Algorithms in all respects. Figure 3 graphically illustrates the implementation of the proposed optimulation algorithm for the OCM process.

Genetic Algorithms are initialized by codifying the input variables into a chromosome-like structure defining a potential solution for the optimization problem. The chromosome, as a well-organized string composed of properly connected genes, is capable of transferring the genetic information. Each chromosome as a genotype is a codified version of an object as its corresponding phenotype, e.g. a recipe in case of the OCM process.

As mentioned in Stage I, five input variables including Modified Reaction Time (*MRT*), volumetric flow of the gas ($\mathring{V}_{gas}$), inlet methane to oxygen ratio (X_{CH4}/X_{O2}), inlet mole fraction of nitrogen (X_{N2}), and the reaction temperature (*T*) are selected as the main determining factors in the case of the OCM process.

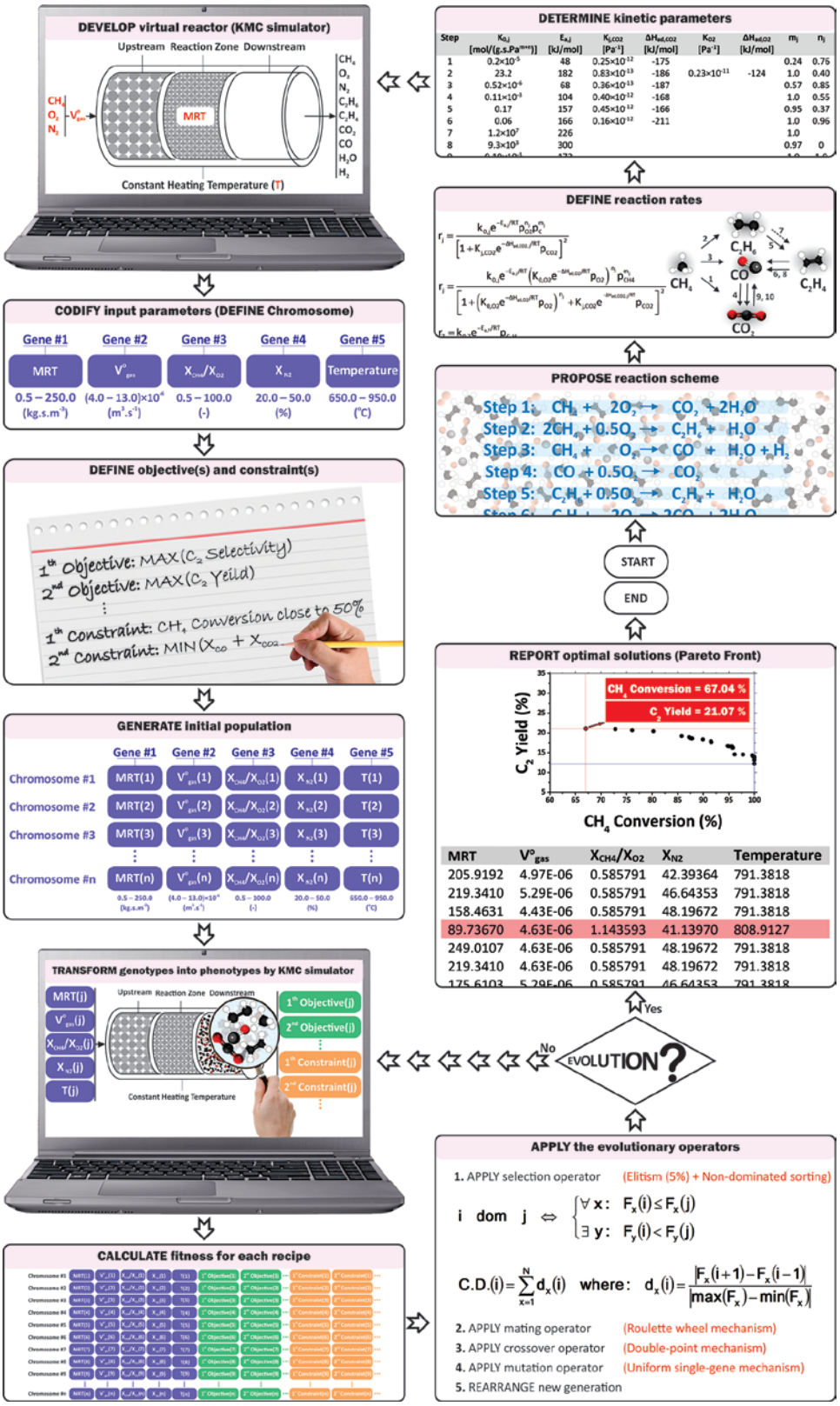

Figure 3. Graphical flowchart illustrating the implementation of the developed 'optimulation' algorithm.

As clearly observed in the box 'CODIFY input parameters (DEFINE chromosome)' of Figure 3, an appropriate chromosome-like structure is designed in which each input variable occupies a unique position (i.e. a gene) in the order given. In the current study, taking into consideration the experimental range of reaction conditions applied in the experiments by Stansch et al.[53], the potential search space considered for each input variable is represented in Table 2. Obviously, changing the potential variation ranges for input variables, NSGA-II can still handle the Optimulation of OCM process for the new search space.

Table 2. The predefined search space for determining input variables.[53]

Input Variables	**Potential Values**		**Unit**
	Low Value	High Value	
Modified Reaction Time (*MRT*)	0.5	250.0	($kg.s.m^{-3}$)
Volumetric flow of the gas ($\mathring{V}_{gas}$)	4.0×10^{-6}	13.0×10^{-6}	($m^3.s^{-1}$)
Inlet Methane to Oxygen ratio (X_{CH4}/X_{O2})	0.5	100.0	(-)
Inlet mole fraction of Nitrogen (X_{N2})	20.0	50.0	(%)
Reaction Temperature (*T*)	650.0	950.0	(^oC)

Having defined the genes, a preset number (of chromosomes) is generated randomly as the initial population. It is worth mentioning that in all Genetic Algorithms the initial population is generated randomly. In other words, new generations are produced via genetic operators capable of combining chromosomes and manipulating genes in order to evolve the population towards optimal solutions.

Having generated the initial population, the optimizer initializes the evaluation process by calculating/quantifying the competencies of chromosomes and assigning fitness value(s) to each chromosome one by one. In all optimizations based on Computational Intelligence techniques, the competencies of potential solutions are quantitatively assessed by definition and application of one or more proper fitness function(s). As graphically illustrated in Figure 3, the developed KMC simulator plays the role of a specific fitness function in the proposed Optimulation methodology. In fact, the optimizer separately recalls the KMC simulator for each chromosome to virtually imitate the OCM

process considering the compositional and operational conditions dictated by that chromosome. Obviously, the outputs calculated and reported via the KMC simulator are collected and stored as fitness values for different chromosomes. Afterwards, the new generation is produced applying genetic operators including selection, crossover, and mutation operators. A brief description of the main genetic operators implemented in the current study is given in what follows.

The selection operator is one of the most important genetic operators in all Genetic Algorithm techniques. It suggests the best chromosomes to be transferred to the next generations for construction of better solutions. In single-objective optimizations, the chromosomes are generally ordered from the most qualified to the less fit according to the calculated fitness values. Choosing one of the available selection mechanisms, including 'merge, sort, truncate', 'elitism', 'roulette wheel', or 'tournament', the satisfactory chromosomes are extracted thereafter. As noted above, the main difference between NSGA-II and other conventional single-objective Genetic Algorithms is the mechanism of sorting potential solutions. In fact, within NSGA-II, chromosomes are appropriately sorted in a multi-objective optimization framework. A domination concept puts the chromosomes into order mainly by the application of two criteria, i.e. the 'quality' and 'diversity' of the solutions. The first criterion clusters the solutions into classes named Pareto fronts, while the second one separately sorts the members of each Pareto front according to their fitness values.

To categorize the chromosomes based on the quality of the solutions, the domination concept is applied. If all objectives should be minimized mutually, then the domination concept is mathematically expressed as Equation 13. According to this equation, a chromosome, e.g. chromosome *i*, dominates another chromosome, e.g. chromosome *j*, if it is not worse than this chromosome in all predefined objectives and definitely better in at least one objective.

$$i \quad dom \quad j \quad \Leftrightarrow \quad \begin{cases} \forall\, x: & F_x(i) \le F_x(j) & x = 1,2,3...,N_{obj} \\ \exists\, y: & F_y(i) < F_y(j) & y \in \{1,2,3...,N_{obj}\} \end{cases} \tag{15}$$

where $F_x(i)$ is the fitness value of chromosome i in objective x and N_{obj} is the total number of predefined objectives.

Having compared all possible pairs of solutions, the selection operator assigns a number or rank to each chromosome based on the dominations. Afterwards, the chromosomes are properly classified into a set of Pareto fronts. It is obvious that the non-dominated chromosomes are placed in the first Pareto front while the second Pareto front hosts those chromosomes dominated once by the members in the first front, and the front construction goes on. The chromosomes in the first front, then, are given a rank value of 1, those in the second front are assigned the rank value of 2, and so on.

The second criterion completes the sorting process via evaluating the diversity of solutions in all Pareto fronts individually. Essentially, the members of each Pareto front are put into order by calculating the so called 'Crowding Distance' for each chromosome. This index essentially measures the proximity of a chromosome to its neighbors in a given Pareto front. Those solutions located in a less crowded region, i.e. a region with a larger average crowding distance, have better diversity and are more preferable. The crowding distance of chromosome i, $C.D.(i)$, is defined as follows:

$$C.D.(i) = \sum_{x=1}^{N_{obj}} d_x(i) \quad where: \quad d_x(i) = \frac{\left|F_x(i+1) - F_x(i-1)\right|}{\left|Max(F_x) - Min(F_x)\right|} \tag{16}$$

In Equation (16), $d_x(i)$ is the crowding distance of chromosome i with respect to objective x. Also, $Min(F_x)$ and $Max(F_x)$ are the minimum and maximum values of objective x, respectively.

Having sorted the chromosomes based on the quality and diversity criteria, the optimization algorithm picks out a preset number of the fittest chromosomes to be transferred to the next generation for offspring production. In this stage, the preset amount of crossover rate dictates the number of chromosomes to be selected.

The winner chromosomes are subsequently utilized to generate new members to be substituted by refused chromosomes of the previous generation; this is accomplished by two well-known powerful intelligent genetic operators, i.e. crossover and mutation. Both operators are stochastic search algorithms but their mechanism and implementation are quite different. Crossover is mainly an expert exploitation tool, while mutation is applied for exploration. Put simply, the crossover operator receives two chromosomes as parents and generates two new chromosomes as offspring, which are similar to the parents. Therefore, the crossover operator seeks the promising regions in the hope of finding superior solutions, i.e. local optima. On the other hand, mutation has an effect on a single chromosome and changes it into a new chromosome, which may or may not be in the current population. Thus, the mutation operator seeks unexplored regions to guarantee that all regions of the search space are thoroughly explored and the search is not confined to limited regions. Obviously, the rate and type of crossover and mutation can be regulated depending on the problem under study.

To apply the crossover operator, the transferred chromosomes from the previous generation should be set up into mating pairs as potential parents to generate the offspring. For the chromosomes to mate, different mechanisms including 'best-best', 'best-worst', 'random', 'roulette wheel', and 'tournament' can be employed. After defining the recombination mechanism, the crossover operator is applied on mated chromosomes. Several types of crossover operators exist, among which single- and multi-point crossover operators are the most popular.

Applying the crossover operator on potential mating pairs and generating the offsprings, the mutation operator manipulates some of the newcomers. The number of offspring chromosomes elected for mutation is determined by the mutation rate. In the first step, the mutation candidates are chosen randomly. Then, one or more genes of each selected chromosomes are manipulated by the mutation operator. It should also be noted that the gene(s) are specified in a stochastic manner for the mutation process. Generally, the value of a selected gene for mutation is randomly replaced by another value among the

minimum and maximum preset values of that gene. The mutated chromosomes are completely replaced by the ones they are originated from.

The evolutionary optimization process is repeated by calculating fitness values of the new population. It stops whenever one or more evolved solutions satisfy the predefined target(s). The values of the parameters used for evolutionary optimization by NSGA-II are given in Supporting Information (see Table S1). Note that the initial population size, crossover rate, mutation rate, and the maximum number of iterations were set to be 500, 50.00%, 15.00%, and 100, respectively.

Taking the aforementioned computational algorithm into account (Figure 3), an optimizer based on NSGA-II was written in Pascal programming language (Lazarus 1.6.4 IDE) and compiled into 64-bit executable using FPC 3.0.2. The optimizer was capable of recalling the KMC simulator developed in Stage I to send codified chromosomes and receive the simulation outputs in a swift manner. The Mersenne Twister pseudorandom number generator was used to produce the required random numbers for the optimulation processes.[69] The random number generation subroutine satisfies the tests of uniformity and serial correlation with high resolution. The cycle length of the random number generator was 2^{19937}-1.

Optimulations were performed on a desktop computer with Intel Core i7-3770K (3.50 GHz), 32 GB of memory (2133 MHz), under Windows 7 Ultimate 64-bit operating system. The runtime was approximately 18 hours for the most complicated optimulation case studies.

3. RESULTS AND DISSCUSION

To evaluate the performance of the developed optimulation algorithm effectively, it is of great importance to verify the accuracy of the developed KMC simulator first. Hence, the established simulator has been put into practice at several compositional and operational conditions and the simulation outputs have been compared with reliable data available in the literature.[52] Furthermore, to appropriately illustrate the outstanding capabilities of the designed optimulation algorithm, it has been implemented to handle the optimization

of the OCM process as an intricate chemical reaction engineering case study. To do this, two different classes of problems have been investigated. The first class, i.e. part A, is considered to investigate aspects of the conventional OCM process consisting of one reaction zone. Different scenarios were defined in part A to practically display the power and versatility of the optimulation algorithm in challenging single- and multi-objective optimization problems (8 case studies). On the other hand, more complicated optimization scenarios were designed to represent the uniqueness of the proposed algorithm. Accordingly, in part B, a multi-stage reactor is optimized in an attempt to explore the possibility of improving the OCM process.

3.1. Verification of the developed KMC simulator

To utilize the developed KMC simulator in the proposed optimulation framework, it is of great importance to appropriately evaluate the precision of its predictions. To do so, the OCM simulator was put into practice to handle the set of reactions under the same conditions reported by Eppinger et al.[52] The simulation outputs, including methane conversion and C_2 selectivity, were calculated and compared with those measured by the research group. It should be noted that the dilution ratio (*DR*) and the initial mole fraction of nitrogen (X_{N2}) were set to be 6.00 and 0.30, respectively. The dilution ratio is defined as the ratio of the mass of quartz sand to that of the catalyst. The developed KMC simulator was capable of successfully predicting the outputs reported for all 15 scenarios in the literature. All calculated errors were less than 2.00%.

3.2. Part A: Optimulation of simple scenarios

The capabilities of the proposed optimulation algorithm were investigated in detail via several single- and multi-objective optimization scenarios. In the case of single-objective problems, the algorithm looked for a specific target, while several objectives and/or constraints were simultaneously satisfied in case of multi-objective scenarios. It is worth mentioning that constraints can be applied both on input variables and responses.

Three different single-objective optimization scenarios (Cases I, II, and III) were defined to evaluate the capabilities of the proposed optimulation algorithm. The first scenario, Case I, is designed to 'back-calculate' the recipe resulting in a C_2 selectivity of 40%. On the other hand, maximizing C_2H_4 and C_2H_6 yields were considered as the main targets in Cases II and III, respectively. Obviously, the algorithm heuristically explores the predefined search spaces in an attempt to find the most appropriate recipe satisfying the predefined objective in each case. As mentioned in the previous section, each recipe consists of adjusting five factors including *MRT*, $\mathring{V}_{gas}$, X_{CH4}/X_{O2}, X_{N2}, and *T*, which should be optimized according to the preset target for each scenario. To do this, the optimulation computer code randomly generates reaction recipes as its initial population and recalls the developed KMC simulator to virtually carry out the OCM process for all suggested recipes. Applying an intelligent evolutionary algorithm and frequently recalling the KMC simulator (essentially in an on-line mode), the optimizer analyzes the virtually synthesized products to find the optimum recipe satisfying the objective predefined in each scenario.

The optimulation results for the designed single-objective optimization case studies are presented in Table 3. As expected, the algorithm has proposed only one optimal solution for each single-objective scenario. The optimal recipe and the detailed composition of the final products are separately reported for each case study. As can be seen, the intelligent optimizer has attempted to solely satisfy the predefined target in each case. In Case I, for instance, the optimizer has explored the preset search space to find the best recipe capable of minimizing the predefined objective, i.e. *Minimize* $|C_2$ selectivity – 40%$|$. Although the proposed solution has successfully satisfied the target, the procedure did not have any control on other reaction outputs, especially CH_4 conversion and C_2 yield. This can be expected, since the optimizer only attempts to evolve the potential solutions of each generation towards the recipes which exhibit C_2 selectivity close to 40%. In other words, the algorithm sorts and elects the elite members (recipes) of each generation based on whether they can minimize the predefined objective, i.e. *Min*$|C_2$ selectivity – 40%$|$. The proposed recipe for Case I is *MRT*: 201.99 kg.s.m^{-3}, $\mathring{V}_{gas}$: 8.29×10^{-6} m^3.s^{-1}, X_{CH4}/X_{O2}: 2.40 (-), X_{N2}: 24.62%, and *T*: 772.93 ^{o}C. Subsequently, the optimal solution was

fed into the KMC simulator to virtually imitate the OCM process and calculate the composition of the final products (see Table 3).

The optimulation algorithm has successfully suggested two distinct recipes for Cases II and III, i.e. for the maximization of C_2H_4 and C_2H_6 yields. More interestingly, the maximum attainable values of C_2H_4 yield (17.64%) and C_2H_6 yield (8.12%) have occurred at *MRT* values of 213.65 and 7.05, respectively. Furthermore, asking for the maximization of the final C_2H_4 and C_2H_6 yields as the optimization target has resulted in recipes leading to methane conversion, C_2 yield, and C_2 selectivity of 71.82, 19.96, and 27.79% (Case II) and 27.21, 13.19, and 48.47% (Case III), respectively. The optimulation algorithm was capable of precisely handling all single-objective optimizations in a computationally cost effective manner. The execution time for each single-objective case study was approximately less than 2.4 hours.

Table 3. Optimulation results obtained for single-objective optimization case studies.

	Single-Objective Scenarios		
	Case I	**Case II**	**Case III**
Optimal Recipe			
MRT (kg.s.m^{-3}):	201.99	213.65	7.05
$\mathring{V}_{gas}$ (m^3.s^{-1}):	8.29×10^{-6}	6.08×10^{-6}	4.06×10^{-6}
X_{CH4}/X_{O2} (-):	2.40	1.01	3.66
X_{N2} (%):	24.62	31.74	48.63
T (^{o}C):	772.93	811.17	854.16
Final Products			
X_{CH4} (%):	31.71	9.25	28.97
X_{O2} (%):	7.59×10^{-8}	5.74×10^{-7}	5.29×10^{-2}
X_{N2} (%):	23.55	30.23	47.97
X_{C2H6} (%):	1.31	0.38	1.62
X_{C2H4} (%):	2.53	2.90	1.01
X_{CO2} (%):	9.40	14.56	3.98
X_{CO} (%):	2.12	2.46	1.60
X_{H2O} (%):	21.50	32.78	12.08
X_{H2} (%):	7.89	7.44	2.72
Reaction Outputs			
CH_4 conversion (%):	37.69	71.82	27.21
C_2H_4 yield (%):	9.93	**17.64**	5.07
C_2H_6 yield (%):	7.14	2.32	**8.12**
C_2 yield (%):	15.07	19.96	13.19
C_2 selectivity (%):	**39.99**	27.79	48.47

In addition to the above single-objective scenarios, several objectives and/or constraints were defined simultaneously in each of the more interesting and demanding multi-

objective optimizations. To challenge the developed optimulation algorithm with more complex problems, three multi-objective optimization case studies were tackled, i.e. Cases IV, V, and VI. Each case study had more than one objectives/constraints to be satisfied. In Case IV, methane conversion and C_2 yield were to be maximized simultaneously. On the other hand, in Case V, the algorithm was supposed to satisfy the same objectives (predefined in Case IV) but now with taking the preset values of X_{CH4}/X_{O2} and X_{N2} into account. It is clear that presetting the values of X_{CH4}/X_{O2} and X_{N2} plays the role of two constraints via confining the algorithm to recognize and pick out only those solutions simultaneously maximizing methane conversion and C_2 yield around the preset values for the mentioned input variables. It is worth mentioning that three separate case studies (Cases V-0.5, V-5, and V-50) were designed in Case V. For all cases, the value of X_{N2} was set to be 41.13%, while distinct values of X_{CH4}/X_{O2} including 0.50, 5.00, and 50.00, were considered, respectively. The algorithm was also tested to handle another complicated task in Case VI. According to the last scenario, the algorithm should attempt to find solutions resulting in maximum C_2 selectivity at methane conversion of 75%. Clearly, presetting the methane conversion at 75% acts as a constraint on a response. This restricts the algorithm to consider only those solutions maximizing C_2 selectivity around the mentioned methane conversion. It should be emphasized that there is no limitation on the number of predesigned objectives and constraints. The selected scenarios are just several examples to seriously challenge and precisely evaluate/investigate the capabilities of the proposed optimulation algorithm.

Figure 4 illustrates the optimization results for the targets defined in Case IV. In contrast to single-objective scenarios, the multi-objective optimizations result in multiple solutions, known as Pareto optimal solutions. In this case, the Optimulation algorithm has successfully suggested 37 solutions satisfying the preset targets. In fact, 37 members of the last population were placed in the first Pareto front as non-dominated solutions. As mentioned previously in the model development section, the initial population size was set to have 500 members (potential solutions or recipes) and the maximum number of iterations of the algorithm was set to 100. Therefore, the optimulation algorithm has

recalled the developed KMC simulator 50,000 times in order to examine 500 potential recipes one-by-one at each epoch in an intelligent evolutionary manner. In the last epoch, 37 out of 500 members of the last generation have successfully satisfied the primary criterion of domination concept and placed in the first Pareto front. According to Figure 4, the obtained recipes were distributed between two extreme solutions specified by the intersections of the red and blue lines, respectively. The former, i.e. the solution represented by the red dot, has been capable of achieving the maximum C_2 yield, whilst the latter, at the intersection of the blue lines, represents the solution resulted in the maximum attainable methane conversion.

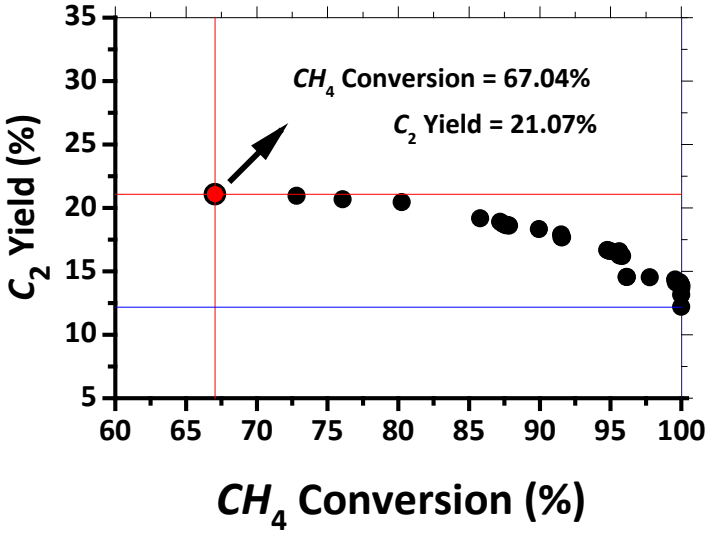

Figure 4. The Pareto optimal front for the multi-objective simulation/optimization of OCM process proposed by the Optimulation algorithm for Case IV.

Table S2 in Supporting Information provides detailed information on the 37 solutions shown in Figure 4 and proposed by the optimulation code. These solutions, located in the first Pareto front, were separated and stored because of being non-dominated. Apparently, all solutions have been successful in simultaneous maximization of methane conversion and C_2 yield. The first column of Table S2 represents the solution number stored. The second to sixth columns represent the recipes proposed by the optimulation algorithm, i.e., the values of the compositional and operational adjustable factors

described in previous sections. The seventh and eighth columns give the outputs of the OCM process for each proposed recipe, i.e. methane conversion and C_2 yield, respectively. Furthermore, and even more importantly, the ninth and tenth columns host the values of the first and second criteria of the domination concept utilized by the intelligent optimizer. The former, entitled 'Ranking', is calculated based on the quality of the solutions, which classifies solutions in different Pareto fronts. Being located in the first Pareto front, all solutions are acceptable and given a rank value of 1. The latter, i.e. *C.D*. column, represents the diversity of the solutions calculated and assigned based on the crowding distance equation for all solutions located in each Pareto front. The second criterion is capable of sorting the solutions isolated in different Pareto fronts separately. The solutions scoring higher crowding distance values are more preferable. Obviously, Solutions 1 and 2 scoring the highest amounts of crowding distance, i.e. infinity (inf.), have been ranked at the top. Interestingly, these are the solutions positioned at the intersections of the blue and red lines in Figure 4. Solution 1 has resulted in maximum attainable methane conversion of 100%, whereas maximum C_2 yield (of 21.078%), has been achieved by Solution 2 (the red dot in Figure 4).

The optimal recipe, detailed composition of final products, and reaction outputs corresponding to the specific solution are reported in Table 4. As can be observed, to simultaneously maximize methane conversion and C_2 yield, the reaction input variables including *MRT*, $\mathring{V}_{gas}$, X_{CH4}/X_{O2}, X_{N2}, and *T* should be set at 89.73 kg.s.m^{-3}, 4.63×10^{-6} m^3.s^{-1}, 1.14 (-), 41.13%, and 808.91 ^{o}C, respectively. This resulted in methane conversion, C_2 yield, and C_2 selectivity of 67.04%, 21.07%, and 31.43%, respectively.

In Case V, the optimulation algorithm should simultaneously satisfy the same objectives but without being allowed to change the preset values of X_{CH4}/X_{O2} and X_{N2}, i.e. two out of five predefined genes (input variables) in the proposed chromosome structure (potential recipe). As mentioned earlier, three distinct scenarios were defined in Case V including V-0.50, V-5.00, and V-50.0. The X_{N2} value was set to be 41.13% (the optimal value obtained in Case IV) in all scenarios, while the X_{CH4}/X_{O2} ratio was set to be 0.50, 5.00, and 50.00 in the case of V-0.50, V-5.00, and V-50.0, respectively. As can be observed from Table 4, the

specific constraints have resulted in different recipes. Interestingly, the optimal values of *MRT* and $\mathring{V}_{gas}$ have been continuously declining from Case V-0.50 to Case V-50.0, while the optimal reaction temperature has increased. The maximum methane conversion and C_2 yield obtained for these scenarios are (89.76% and 12.04%), (23.00% and 13.15%), and (4.62% and 4.01%), respectively.

Finally, in Case VI, the Optimulation algorithm should intelligently explore the search space to find the recipes leading to maximum C_2 selectivity at methane conversion of 75.00% (one objective and one constraint to be simultaneously satisfied). To handle Case VI appropriately, the defined constraint was initially converted into an objective as follows:

$$CH_4 \text{ conversion} \rightarrow 75.00\% \equiv Min(|CH_4 \text{ conversion} - 75.00\%|) \quad (17)$$

Hence, two objectives including maximization of C_2 selectivity and minimization of ($|CH_4$ conversion – 75.00%|) should be simultaneously satisfied in Case VI. The optimulation algorithm was put into practice to handle the scenario as a two-objective optimization problem. Figure 5 represents the Pareto optimal front (82 solutions) obtained for Case VI.

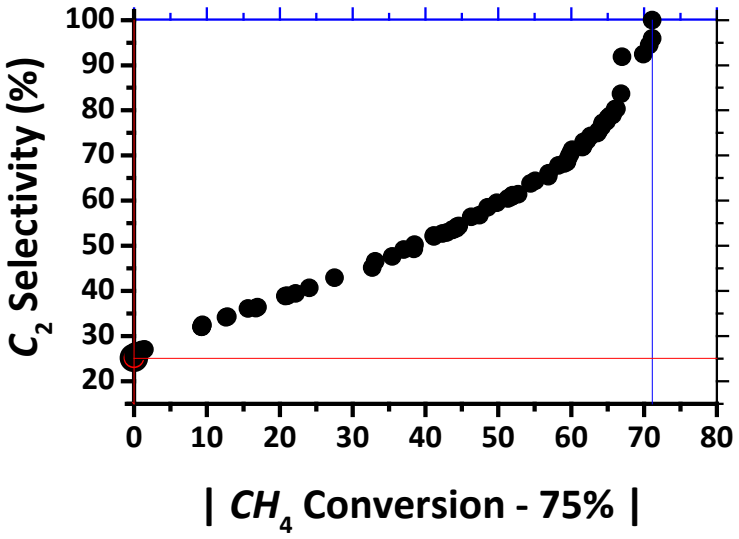

Figure 5. The Pareto optimal front for the multi-objective simulation/optimization of OCM, Case VI.

In this case, the red dot (located at the intersection of the red lines) was selected as the optimal solution. It has the closest methane conversion (75.06%) to the preset conversion value. The maximum attainable C_2 selectivity was 25.64% when the methane conversion was intentionally preset at 75.00%. The optimal recipe corresponding to this solution along with reaction outputs and composition of final products are cited in the last column of Table 4. The optimal reaction input variables were predicted to be *MRT*: 51.03 kg.s.m^{-3}, $\mathring{V}_{gas}$: 4.48×10^{-6} m^3.s^{-1}, X_{CH4}/X_{O2}: 0.94 (-), X_{N2}: 24.98%, and *T*: 824.52 ^{o}C. It should be noted that although the solution positioned at the intersection of the blue lines of Figure 5 resulted in C_2 selectivity of about 100%, it cannot be nominated as the optimal solution due to the fact that it exhibits a methane conversion of only 3.87%.

Table 4. Optimulation results obtained for multi-objective optimization case studies.

		Multi-Objective Scenarios				
		Case IV	**Case V-0.5**	**Case V-5**	**Case V-50**	**Case VI**
Optimal Recipe						
	MRT (kg.s.m^{-3}):	89.73	45.39	14.78	1.04	51.03
	$\mathring{V}_{gas}$ (m^3.s^{-1}):	4.63×10^{-6}	4.50×10^{-6}	4.13×10^{-6}	4.09×10^{-6}	4.48×10^{-6}
	X_{CH4}/X_{O2} (-):	1.14	**0.50**	**5.00**	**50.00**	0.94
	X_{N2} (%):	41.13	**41.13**	**41.13**	**41.13**	24.98
	T (^{o}C):	808.91	788.77	808.07	948.77	824.52
Final Products						
	X_{CH4} (%):	10.10	1.92	37.31	55.21	8.63
	X_{O2} (%):	1.60×10^{-6}	11.69	1.23×10^{-6}	4.93×10^{-4}	3.64×10^{-2}
	X_{N2} (%):	39.49	39.37	40.63	41.25	23.80
	X_{C2H6} (%):	0.55	0.15	1.83	1.01	0.44
	X_{C2H4} (%):	2.62	0.98	1.36	0.15	2.89
	X_{CO2} (%):	11.74	13.42	3.55	0.07	16.94
	X_{CO} (%):	2.07	1.17	1.23	0.28	2.39
	X_{H2O} (%):	26.93	23.75	11.06	1.88	37.33
	X_{H2} (%):	6.50	7.55	3.04	0.14	7.55
Reaction Outputs						
	CH_4 conversion (%):	**67.04**	**89.76**	**23.00**	**4.62**	**75.06**

C_2 yield (%):	**21.07**	**12.04**	**13.15**	**4.01**	19.24
C_2 selectivity (%):	31.43	13.41	57.17	86.79	**25.64**

3.3. Part B: Optimulation of intricate scenarios

In this part, several complex optimization scenarios were designed to seriously challenge and test further the optimulation algorithm. To do this, it was considered that the OCM process can take place in a sequence of *n* consecutive reaction zones, i.e. a multi-stage reactor (see Figure 6). It was assumed that the reaction temperature is similar in all reaction zones while each one has its own *MRT*, i.e. each zone has a specific residence time (t_R) and height of the catalytic packed bed (H_R) value. Also, the final products of the i^{th} reaction zone enter the $(i+1)^{th}$ reaction zone. Furthermore, at the entrance of each reaction zone, a fresh feed with volumetric flow of $\mathring{V}_{gas}(i+1)$ composed of methane, oxygen, and nitrogen with the mole fractions of $X_{CH4}(i+1)$, $X_{O2}(i+1)$ and $X_{N2}(i+1)$, is fed into the reaction zone to be combined with the outputs of the previous stage. Figure 6 schematically illustrates the configuration of the proposed multi-stage OCM reactor along with all design factors. In this part, a complicated multi-objective optimization problem has to be addressed, which is very hard, if not impossible, to handle by classical deterministic and stochastic optimization methodologies.

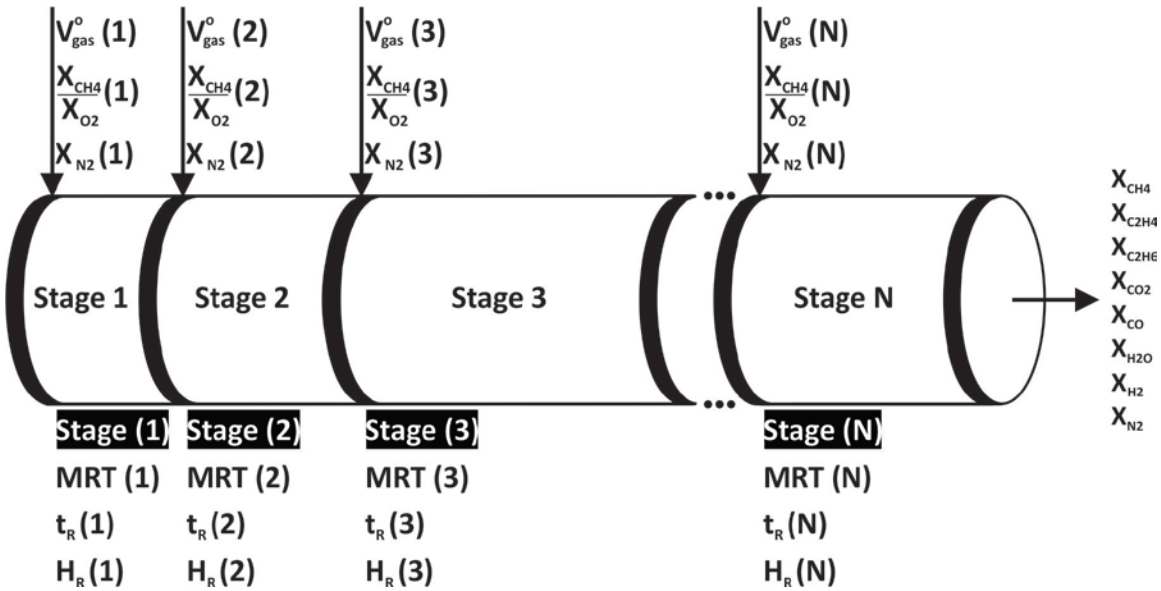

Figure 6. Schematic representation of a multi-stage reactor proposed for Optimulation of OCM process.

Although various objectives and constraints can be defined as optimization targets, it was supposed that simultaneous maximization of methane conversion and C_2 yield are the main targets to be satisfied in part B. Hence, the hybrid algorithm should explore the reaction search space (Table 2) in an attempt to maximize both objectives at the same time.

A very large number of scenarios was considered as possible optimization problems. The main difference between the designed optimization scenarios was the number of assigned reaction zones for the OCM process. Accordingly, the number of reaction zones can vary between 2 and 10. This means that the simplest reactor configuration was considered to have two consecutive reaction zones, i.e. a two-stage OCM reactor, while a more complex one was allowed to have 10 distinct reaction zones, a sequence of 10 consecutive zones. It is clear that in each reaction zone, four (4) manipulated factors should be optimized. Also, the reaction temperature is the common adjustable variable for optimization. Therefore, the proposed reactor configuration for the OCM process with a sequence of n consecutive reaction zones consists of $(4n+1)$ adjustable factors to be optimized through the developed multi-objective optimization tool. In other words, a two-stage reactor has nine (9) variables while a ten-stage one has 41 variables to be selected (adjusted) for optimization.

Each scenario was separately 'optimulated' by the established hybrid simulator/optimizer. The Pareto optimal front obtained for each complex scenario is illustrated in Figure 7. As can be observed, the proposed algorithm was capable of effectively handling the designed optimization problems at all levels of complexity. Obviously, the algorithm has proposed multiple solutions for each scenario located in the first Pareto front (of the last iteration).

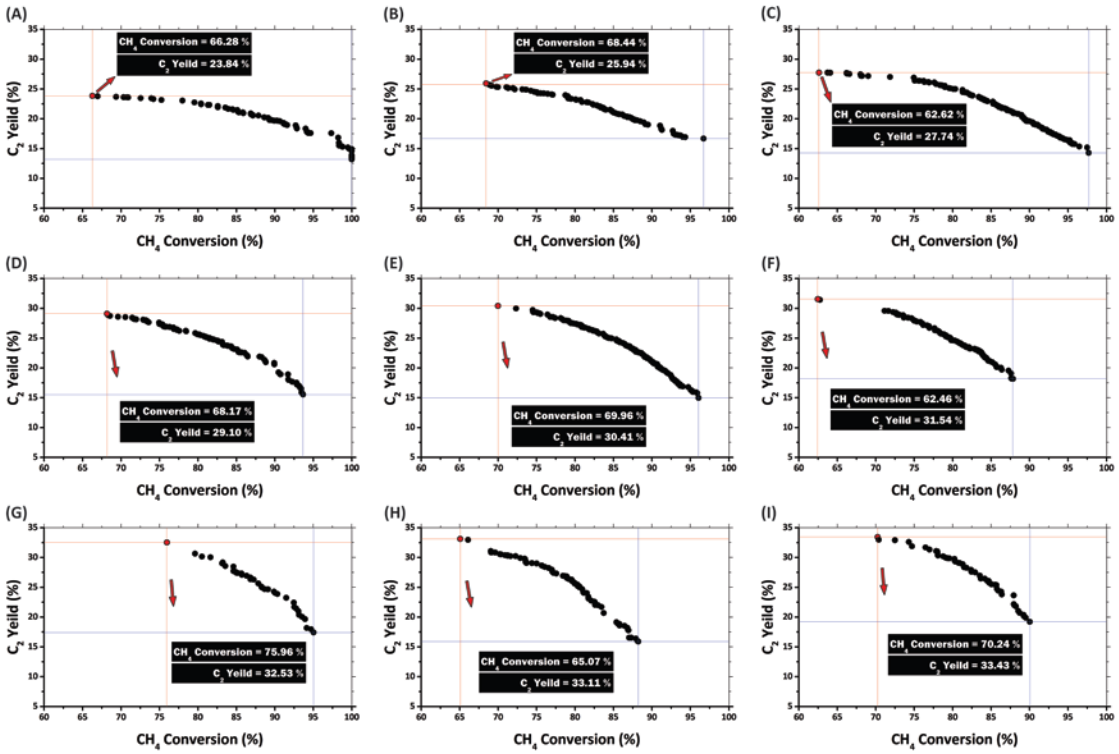

Figure 7. Pareto optimal fronts obtained for the multi-objective optimulations of the OCM process; cases A - I: n = 2-10, respectively.

Among all of the proposed solutions, the two (extreme) ones specified at the intersections of the red and blue lines are practically the most important ones. The solution located at the intersection of the blue lines (of Figure 7) signifies the maximum attainable methane conversion, while the red dot determines the maximum achievable amount of C_2 yield. As mentioned in the previous section, each point in Figure 7 represents a potential solution located at the first Pareto front and is thus connected to a recipe (calculated and reported by the intelligent optimizer). The number of factors constructing a recipe equals to ($4n$+1). As higher C_2 yield values are more favorable in the OCM processes, the obtained recipes corresponding to solutions represented by the red dots are cited in Table S3 in Supporting Information (in other words, applying the listed recipes results in C_2 yields and methane conversions specified by the red dots of Figure 7).

The reaction outputs and the composition of the final products for all multi-objective scenarios (of Figure 7 and Table S3) are reported in Table 5. These have been calculated

via the KMC simulator based on the recipes (red dots in Figure 7) proposed by the optimulation algorithm as optimal solutions.

Table 5. Optimulation results obtained for multi-objective optimizations in the case of the multi-stage OCM reactor.

	Number of Reaction Stages								
Final Products	**2**	**3**	**4**	**5**	**6**	**7**	**8**	**9**	**10**
X_{CH4} (%):	10.00	9.24	13.27	11.59	10.10	15.90	8.32	12.92	11.65
X_{O2} (%):	4.68×10^{-5}	1.01×10^{-4}	1.17×10^{-4}	4.96×10^{-5}	3.47×10^{-4}	1.88×10^{-5}	1.57×10^{-5}	2.34×10^{-5}	8.32×10^{-4}
X_{N2} (%):	42.92	44.16	35.62	30.93	35.73	25.48	32.96	33.08	29.16
X_{C2H6} (%):	0.44	0.47	0.58	0.56	0.43	0.64	0.42	0.45	0.41
X_{C2H4} (%):	3.03	3.19	4.32	4.68	4.63	6.03	4.95	5.74	5.79
X_{CO2} (%):	10.64	10.43	10.63	12.31	11.58	11.31	12.88	10.48	11.92
X_{CO} (%):	1.73	1.58	1.70	1.76	1.57	1.78	1.47	1.48	1.75
X_{H2O} (%):	25.26	25.37	27.52	31.88	30.11	32.15	33.27	29.97	32.93
X_{H2} (%):	5.98	5.56	6.36	6.29	5.85	6.71	5.73	5.88	6.39
Reaction Outputs	**2**	**3**	**4**	**5**	**6**	**7**	**8**	**9**	**10**
CH_4 conversion (%):	66.28	68.44	62.62	68.17	69.96	62.45	75.96	65.07	70.24
C_2 yield (%):	**23.84**	**25.94**	**27.74**	**29.10**	**30.41**	**31.54**	**32.53**	**33.11**	**33.42**
C_2 selectivity (%):	35.97	37.91	44.30	42.69	43.47	50.50	42.82	50.88	47.58

According to the results obtained, the C_2 yield is considerably improved from 23.84 to 33.42% by increasing the number of consecutive reaction zones from 2 to 10, respectively. The variation of the maximum attainable C_2 yield versus the number of consecutive reaction zones is depicted in Figure 8. As can be observed, the influence of the number of reaction zones/stages on C_2 yield is decreased approximately after 7 consecutive reaction zones.

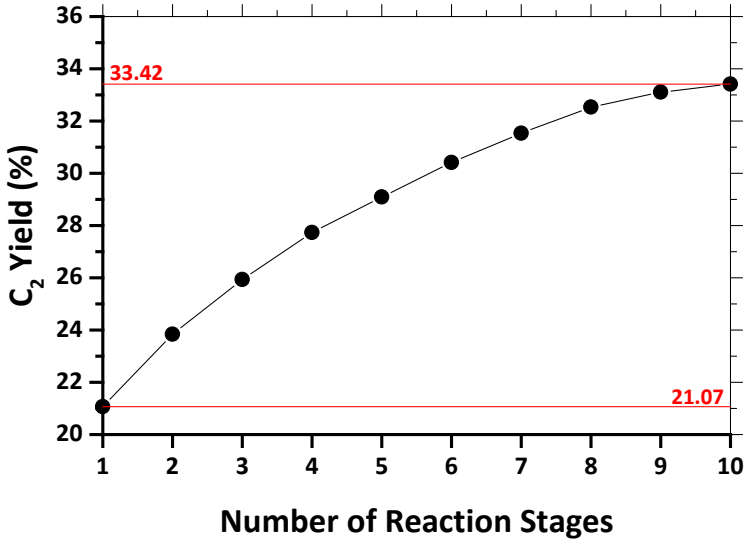

Figure 8. Maximum attainable C_2 yield versus number of proposed reaction zones/stages.

It is obvious that we can apply other input variables to be optimized and/or replace the adjustable factors already considered in this work (Table 2). The desirable manipulated variables can be of different types, including operational or compositional reaction factors, different feeding policies, various reactor configurations and modes of operation, etc. Furthermore, not only can other ranges for selected input variables (adjustable factors) be defined but also different targets (objectives) with or without constraint(s) can be used as the goals of optimulation.

4. CONCLUSION

In the current study, a novel hybrid intelligent computational tool, i.e. 'optimulation' algorithm, was introduced and explained for the first time to effectively handle the simultaneous simulation and optimization of many types of complex reacting systems, including chemical, biological, and macromolecular reactions. The proposed tool was developed based on the amalgamation of the Kinetic Monte Carlo simulation approach (as a well-documented molecular simulation tool) and the Non-dominated Sorting Genetic Algorithm (as the most powerful intelligent multi-objective optimization

technique). The developed algorithm was evaluated in detail with the case of Oxidative Coupling of Methane (a well-known intricate chemical reacting system). The developed computer code based on this optimulation algorithm was capable of successfully handling all defined single- and multi-objective optimization scenarios. The obtained results clearly showed that it is a powerful tool to solve optimization problems of different levels of complexity. Undoubtedly, the established computational framework can be effectively applied by academic and industrial experts to manage a wide variety of types of multi-objective optimization problems for complex reacting systems.

REFERENCES

(1) Mao, Z.; Yang, C. Computational Chemical Engineering - Towards thorough Understanding and Precise Application. *Chin. J. Chem. Eng.* **2016**, 24(8), 945.

(2) Degnan Jr., T. F. Chemical Reaction Engineering Challenges in the Refining and Petrochemical Industries - The Decade Ahead. *Curr. Opin. Chem. Eng.* **2015**, 9, 75.

(3) Woinaroschy, A. A Paradigm-based Evolution of Chemical Engineering. *Chin. J. Chem. Eng.* **2016**, 24(5), 553.

(4) Woinaroschy, A. Chemical Reaction Engineering, Process Design and Scale-up Issues at the Frontier of Synthesis: Flow Chemistry. *Chem. Eng. J.* **2016**, 296, 56.

(5) Kuipers, J. A. M.; van Swaaij, W. P. M. Computational Fluid Dynamics Applied to Chemical Reaction Engineering. *Adv. Chem. Eng.* **1998**, 24, 227.

(6) Blumenberg, B. Chemical Reaction Engineering in Today's Industrial Environment. *Chem. Eng. Sci.* **1992**, 47(9-11), 2149.

(7) Carpenter, K. J. Chemical Reaction Engineering Aspects of Fine Chemicals Manufacture. *Chem. Eng. Sci.* **2001**, 56(2), 305.

(8) Fitzpatrick, D. E.; Ley, S. V. Engineering Chemistry for the Future of Chemical Synthesis. *Tetrahedron* **2017**, https://doi.org/10.1016/j.tet.2017.08.050.

(9) Senkan, S. M. Detailed Chemical Kinetic Modeling: Chemical Reaction Engineering of the Future. *Adv. Chem. Eng.* **1992**, 18, 95.

(10) Xu, J.; Li, X.; Hou, C.; Wang, L.; Zhou, G.; Ge, W.; Li, J. Engineering Molecular Dynamics Simulation in Chemical Engineering. *Chem. Eng. Sci.* **2015**, 121, 200.

(11) Gissinger, J. R.; Jensen, B. D.; Wise, K. E. Modeling Chemical Reactions in Classical Molecular Dynamics Simulations. *Polym. J.* **2017**, 128, 211.

(12) Eyring, H. Quantum Mechanics and Chemical Reactions. *Chem. Rev.* **1932**, 10(1), 103.

(13) Piersall, S. D.; Anderson, J. B. Direct Monte Carlo Simulation of Chemical Reaction Systems: Simple Bimolecular Reactions. *J. Chem. Phys.* **1991**, 95(2), 971.

(14) Mohammadi, Y.; Najafi, M.; Haddadi-Asl, V. Comprehensive Study of Free Radical Copolymerization Using a Monte Carlo Simulation Method, 1. Both Reactivity Ratios Less than Unity. (r_A <1 and r_B <1). *Macromol. Theory Simul.* **2005**, 14(5), 325.

(15) Gillespie, D. T. Exact Stochastic Simulation of Coupled Chemical Reactions. *J. Phys. Chem.* **1977**, 81(25), 2340.

(16) Zhang, X.; Han, B.; Li, Y.; Zhong, B.; Peng, S. Monte Carlo Simulation for Methanol Synthesis on Metal Catalyst in Supercritical *n*-Hexane. *J. Supercrit. Fluids* **2002**, 23(2), 169.

(17) Bashiri, H.; Pourbeiram, N. Biodiesel Production through Transesterification of Soybean Oil: A Kinetic Monte Carlo Study. *J. Mol. Liq.* **2016**, 223, 10.

(18) Saeb, M. R.; Mohammadi, Y.; Ahmadi, M.; Khorasani, M. M.; Stadler, F. J. A Monte Carlo-based Feeding Policy for Tailoring Microstructure of Copolymer Chains: Reconsidering the Conventional Metallocene Catalyzed Polymerization of α-Olefins. *Chem. Eng. J.* **2015**, 274, 169.

(19) Brandão, A. L. T.; Soares, J. B. P.; Pinto, J. C.; Alberton, A. L. When Polymer Reaction Engineers Play Dice: Applications of Monte Carlo Models in PRE. *Macromol. React. Eng.* **2015**, 9(3), 141.

(20) Mohammadi, Y.; Saeb, M. R.; Penlidis, A.; Jabbari, E.; Zinck, P.; Stadler, F. J.; Matyjaszewski, K. Intelligent Monte Carlo: A New Paradigm for Inverse Polymerization Engineering. *Macromol. Theory Simul.* **2018**, https://doi.org/10.1002/mats.201700106.

(21) Khorasani, M. M.; Saeb, M. R.; Mohammadi, Y.; Ahmadi, M. The Evolutionary Development of Chain Microstructure during Tandem Polymerization of Ethylene: A Monte Carlo Simulation Study. *Chem. Eng. Sci.* **2014**, 111, 211.

(22) Slepoy, A.; Thompson, A. P.; Plimpton, S. J. A Constant-Time Kinetic Monte Carlo Algorithm for Simulation of Large Biochemical Reaction Networks. *J. Chem. Phys.* **2008**, 128(20), 205101.

(23) Berry, H. Monte Carlo Simulations of Enzyme Reactions in Two Dimensions: Fractal Kinetics and Spatial Segregation. *Biophys. J.* **2002**, 83(4), 1891.

(24) Mohammadi, Y.; Ahmadi, M.; Saeb, M. R.; Khorasani, M. M.; Yang, P.; Stadler, F. J. A Detailed Model on Kinetics and Microstructure Evolution during Copolymerization of Ethylene and 1-Octene: From Coordinative Chain Transfer to Chain Shuttling Polymerization. *Macromolecules* **2014**, 47, 4778.

(25) Pladis, P.; Meimaroglou, D.; Kiparissides, C. Prediction of the Viscoelastic Behavior of Low-Density Polyethylene Produced in High-Pressure Tubular Reactors. *Macromol. React. Eng.* **2015**, 9(3), 271.

(26) Saeb, M. R.; Mohammadi, Y.; Rastin, H.; Kermaniyan, T. S.; Penlidis, A. Visualization of Bivariate Sequence Length–Chain Length Distribution in Free Radical Copolymerization. *Macromol. Theory Simul.* **2017**, 26(5), 1700041.

(27) Tripathi, A. K.; Sundberg, D. C. A Hybrid Algorithm for Accurate and Efficient Monte Carlo Simulations of Free-Radical Polymerization Reactions. *Macromol. Theory Simul.* **2015**, 24(1), 52.

(28) Meimaroglou, D.; Pladis, P.; Baltsas, A.; Kiparissides, C. Prediction of the Molecular and Polymer Solution Properties of LDPE in a High-Pressure Tubular Reactor Using a Novel Monte Carlo Approach. *Chem. Eng. Sci.* **2011**, 66(8), 1685.

(29) Saeb, M. R.; Mohammadi, Y.; Pakdel, A. S.; Penlidis, A. Molecular Architecture Manipulation in Free Radical Copolymerization: An Advanced Monte Carlo Approach to Screening Copolymer Chains with Various Comonomer Sequence Arrangements", *Macromol. Theory Simul.* **2016**, 25(4), 369.

(30) Sturtevant, N. R.; Bulitko, V. Scrubbing during Learning in Real-time Heuristic Search. *J. Artif. Intell. Res.* **2016**, 57, 307.

(31) Muthukumar, K.; Jayalalitha, S. Optimal Placement and Sizing of Distributed Generators and Shunt Capacitors for Power Loss Minimization in Radial Distribution Networks Using

Hybrid Heuristic Search Optimization Technique. *Int. J. Electr. Power Energy Syst.* **2016**, 78, 299.

(32) Simpson-Porco, J. W.; Bullo, F. Distributed Monitoring of Voltage Collapse Sensitivity Indices. *IEEE Trans. Smart Grid* **2016**, 7(4), 1979.

(33) D'Addona, D. M.; Teti, R. Genetic Algorithm-based Optimization of Cutting Parameters in Turning Processes. *Procedia CIRP* **2013**, 7, 323.

(34) Sjöberg, J.; Zhang, Q.; Ljung, L.; Benveniste, A.; Delyon, B.; Glorennec, P.-Y.; Hjalmarsson, H.; Juditsky, A. Nonlinear Black-Box Modeling in System Identification: A Unified Overview. *Automatica* **1995**, 31(12), 1691.

(35) Fernandes, F. A. N.; Lona, L. M. F. Neural Network Applications in Polymerization Processes. *Braz. J. Chem. Eng.* **2005**, 22(3), 401.

(36) Zhang, J. Batch-to-Batch Optimal Control of a Batch Polymerisation Process based on Stacked Neural Network Models. *Chem. Eng. Sci.* **2008**, 63(5), 1273.

(37) Zhang, J.; Morris, A. J.; Martin, E. B.; Kiparissides, C. Prediction of Polymer Quality in Batch Polymerisation Reactors Using Robust Neural Networks. *Chem. Eng. J.* **1998**, 69(2), 135.

(38) d'Anjou, A.; Torrealdea, F. J.; Leiza, J. R.; Asua, J. M.; Arzamend, G. Model Reduction in Emulsion Polymerization Using Hybrid First-Principles/Artificial Neural Network Models. *Macromol. Theory Simul.* **2003**, 12(1), 42.

(39) Ng C. W.; Hussain, M. A. Hybrid Neural Network - Prior Knowledge Model in Temperature Control of a Semi-batch Polymerization Process. *Chem. Eng. Process. Process Intensif.* **2004**, 43(4), 559.

(40) Gonzaga, J. C. B.; Meleiro, L. A. C.; Kiang, C.; Filho, R. M. ANN-based Soft-sensor for Real-time Process Monitoring and Control of an Industrial Polymerization Process. *Comput. Chem. Eng.* **2009**, 33(1), 43.

(41) Minari, R. J.; Stegmayer, G. S.; Gugliotta, L. M.; Chiotti, O. A.; Vega, J. R. Industrial SBR Process: Computer Simulation Study for Online Estimation of Steady-state Variables Using Neural Networks. *Macromol. React. Eng.* **2007**, 1(3), 405.

(42) Farrell, B. L.; Igenegbai, V. O.; Linic, S. A Viewpoint on Direct Methane Conversion to Ethane and Ethylene Using Oxidative Coupling on Solid Catalysts. *ACS Catal.* **2016**, 6(7), 4340.

(43) Galadima, A.; Muraza, O. Revisiting the Oxidative Coupling of Methane to Ethylene in the Golden Period of Shale Gas: A Review. *J. Ind. Eng. Chem.* **2016**, 37, 1.

(44) Salkuyeh, Y. K.; Adams II, T. A. A Novel Polygeneration Process to Co-produce Ethylene and Electricity from Shale Gas with Zero CO_2 Emissions via Methane Oxidative Coupling. *Energy Convers. Manage.* **2015**, 92, 406.

(45) Alvarez-Galvan, M. C.; Mota, N.; Ojeda, M.; Rojas, S.; Navarro, R. M.; Fierro, J. L. G. Direct Methane Conversion Routes to Chemicals and Fuels. *Catal. Today* **2011**, 171(1), 15.

(46) Tye, C. T.; Mohamed, A. R.; Bhatia, S. Modeling of Catalytic Reactor for Oxidative Coupling of Methane Using La_2O_3/CaO Catalyst. *Chem. Eng. J.* **2002**, 87, 49.

(47) Godini, H. R.; Jaso, S.; Nghiem, S. X.; Görke, O.; Sadjadi, S.; Stünkel, S.; Song, S.; Simon, U.; Schomäcker, R.; Wozny, G. Miniplant-scale Analysis of Oxidative Coupling of Methane Process. *J Oil Gas Petrochem. Technol.* **2015**, 2(1), 57.

(48) Tiemersma, T. P.; Chaudhari, A. S.; Gallucci, F.; Kuipers, J. A. M.; van Sint Annaland, M. Integrated Autothermal Oxidative Coupling and Steam Reforming of Methane. Part 2: Development of a Packed Bed Membrane Reactor with a Dual Function Catalyst. *Chem. Eng. Sci.* **2012**, 82, 232.

(49) Oh, S. C.; Wu, Y.; Tran, D. T.; Lee, I. C.; Lei, Y.; Liu, D. Influences of Cation and Anion Substitutions on Oxidative Coupling of Methane over Hydroxyapatite Catalysts. *Fuel* **2016**, 167, 208.

(50) Pannek, U.; Mleczko, L. Comprehensive Model of Oxidative Coupling of Methane in a Fluidized-bed Reactor. *Chem. Eng. Sci.* **1996**, 51(14), 3575.

(51) Ghose, R.; Hwang, H. T.; Varma, A. Oxidative Coupling of Methane Using Catalysts Synthesized by Solution Combustion Method: Catalyst Optimization and Kinetic Studies. *Appl. Catal., A* **2014**, 472, 39.

(52) Eppinger, T.; Wehinger, G.; Kraume, M. Parameter Optimization for the Oxidative Coupling of Methane in a Fixed Bed Reactor by Combination of Response Surface Methodology and Computational Fluid Dynamics. *Chem. Eng. Res. Des.* **2014**, 92(9), 1693.

(53) Stansch, Z.; Mleczko, L.; Baerns, M. Comprehensive Kinetics of Oxidative Coupling of Methane over the La_2O_3/CaO Catalyst. *Ind. Eng. Chem. Res.* **1997**, 36, 2568.

(54) Simon, Y.; Baronnet, F.; Marquaire, P.-M. Kinetic Modeling of the Oxidative Coupling of Methane. *Ind. Eng. Chem. Res.* **2007**, 46, 1914.

(55) Vatani, A.; Jabbari, E.; Askarieh, M.; Torangi, M. A. Kinetic Modeling of Oxidative Coupling of Methane over Li/MgO Catalyst by Genetic Algorithm. *J. Nat. Gas Sci. Eng.* **2014**, 20, 347.

(56) Zhang, Z.; Guo, Z.; Ji, S. Numerical Simulation of Fixed Bed Reactor for Oxidative Coupling of Methane over Monolithic Catalyst. *Chin. J. Chem. Eng.* **2015**, 23(10), 1627.

(57) Farsi, A.; Moradi, A.; Ghader, S.; Shadravan, V.; Manan, Z. A. Kinetics Investigation of Direct Natural Gas Conversion by Oxidative Coupling of Methane. *J. Nat. Gas Sci. Eng.* **2010**, 2, 270.

(58) Daneshpayeh, M.; Khodadadi, A.; Mostoufi, N.; Mortazavi, Y.; Sotudeh-Gharebagh, R.; Talebizadeh, A. Kinetic Modeling of Oxidative Coupling of Methane over $Mn/Na_2WO_4/SiO_2$ Catalyst. *Fuel Process. Technol.* **2009**, 90, 403.

(59) Zhang, Z.; Ji, S. Numerical Simulation of Particle/Monolithic Two-stage Catalyst Bed Reactor with Beds-interspace Distributed Dioxygen Feeding for Oxidative Coupling of Methane. *Comput. Chem. Eng.* **2016**, 90, 247.

(60) Marsaglia, G. Random Number Generators. *J. Mod. Appl. Stat. Methods* **2003**, 2(1), 2.

(61) Shukla, P. K.; Deb, K.; Tiwari, S. Comparing Classical Generating Methods with an Evolutionary Multi-objective Optimization Method. *Third International Conference on Evolutionary Multi-Criterion Optimization* **2005**, 3410, 311.

(62) Greiner, D.; Galván, B.; Périaux, J.; Gauger, N.; Giannakoglou, K.; Winter, G. Advances in Evolutionary and Deterministic Methods for Design, Optimization and Control in Engineering and Sciences; Springer International Publishing: Switzerland, 2015.

(63) Russell, S. J.; Norvig, P. Artificial Intelligence: A Modern Approach; Prentice Hall: New Jersey, 2009.

(64) Garshasbi, S.; Kurnitski, J.; Mohammadi, Y. A Hybrid Genetic Algorithm and Monte Carlo Simulation Approach to Predict Hourly Energy Consumption and Generation by a Cluster of Net Zero Energy Buildings. *Appl. Energy* **2016**, 179, 626.

(65) Baghaei, B.; Saeb, M. R.; Jafari, S. H.; Khonakdar, H. A.; Rezaee, B.; Goodarzi, V.; Mohammadi, Y. Modeling and Closed-loop Control of Particle Size and Initial Burst of PLGA Biodegradable Nanoparticles for Targeted Drug Delivery. *J. Appl. Polym. Sci.* **2017**, 134(33), 45145.

(66) Azari, R.; Garshasbi, S.; Amini, P.; Rashed-Ali, H.; Mohammadi, Y. Multi-objective Optimization of Building Envelope Design for Life Cycle Environmental Performance. *Energy Build.* **2016**, 126, 524.

(67) Kannan, S.; Baskar, S.; McCalley, J. D.; Murugan, P. Application of NSGA-II Algorithm to Generation Expansion Planning. *IEEE Trans. Power Syst.* **2009**, 24(1), 454.

(68) Hosseinnezhad, M.; Saeb, M. R.; Garshasbi, S.; Mohammadi, Y. Realization of Manufacturing Dye-sensitized Solar Cells with Possible Maximum Power Conversion Efficiency and Durability. *Sol. Energy* **2017**, 149, 314.

(69) Matsumoto, M.; Nishimura, T. Mersenne Twister: A 623-dimensionally Equidistributed Uniform Pseudo-random Number Generator. *ACM Trans. Model. Comput. Simul.* **1998**, 8(1), 3.

For Table of Contents Only

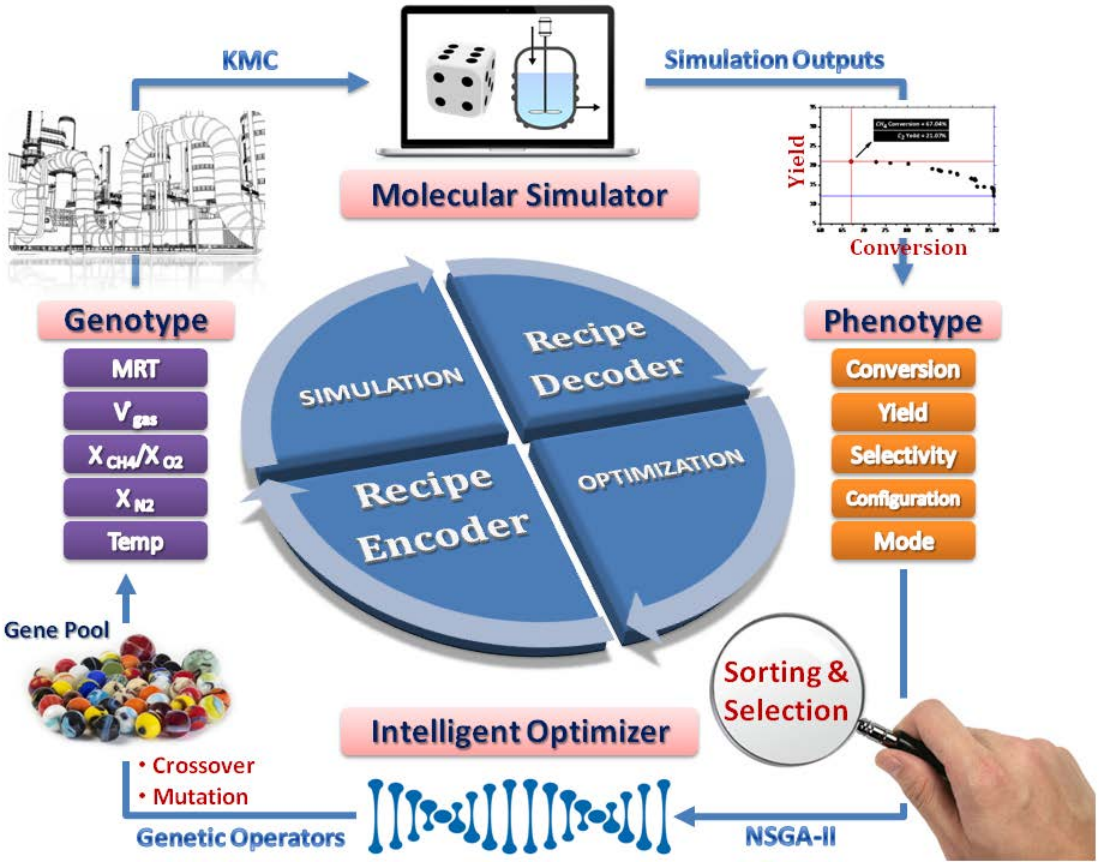

ASSOCIATED CONTENT

Supporting Information Available (free of charge via the internet at http: //pubs.acs.org): Additional information on (1) the parameter values for multi-objective optimization by NSGA-II (Table S1), (2) details of Pareto optimal solutions obtained in the last iteration for Case IV (Table S2), and (3) optimal solutions obtained for the optimization scenarios in the case of the multi-stage OCM reactor (Table S3).

FINANCIAL INTEREST

The authors declare no competing financial interest.